

ARNet: Automatic Refinement Network for Noisy Partial Label Learning

Zheng Lian, Mingyu Xu, Lan Chen, Licai Sun, Bin Liu, and Jianhua Tao, *Senior Member, IEEE*

Abstract—Partial label learning (PLL) is a typical weakly supervised learning, where each sample is associated with a set of candidate labels. The basic assumption of PLL is that the ground-truth label must reside in the candidate set. However, this assumption may not be satisfied due to the unprofessional judgment of the annotators, thus limiting the practical application of PLL. In this paper, we relax this assumption and focus on a more general problem, noisy PLL, where the ground-truth label may not exist in the candidate set. To address this challenging problem, we further propose a novel framework called “Automatic Refinement Network (ARNet)”. Our method consists of multiple rounds. In each round, we purify the noisy samples through two key modules, i.e., noisy sample detection and label correction. To guarantee the performance of these modules, we start with warm-up training and automatically select the appropriate correction epoch. Meanwhile, we exploit data augmentation to further reduce prediction errors in ARNet. Through theoretical analysis, we prove that our method is able to reduce the noise level of the dataset and eventually approximate the Bayes optimal classifier. To verify the effectiveness of ARNet, we conduct experiments on multiple benchmark datasets. Experimental results demonstrate that our ARNet is superior to existing state-of-the-art approaches in noisy PLL. **Our code will be made public soon.**

Index Terms—Automatic Refinement Network (ARNet), noisy partial label learning, noisy sample detection, label correction, multi-round refinement.

1 INTRODUCTION

PARTIAL label learning (PLL) [1], [2], also called ambiguous label learning [3], [4] and superset label learning [5], [6], is a specific type of weakly supervised learning. In PLL, each sample is associated with a set of candidate labels, only one of which is the ground-truth label. Due to the high monetary cost of accurately labeled data, PLL has become an active research area in many tasks such as web mining [7], object annotation [8] and ecological informatics [9].

Unlike supervised learning, the ground-truth label is concealed in the candidate set and invisible to PLL [10], [11], which increases the difficulty of model training. Researchers propose various approaches to address this problem. These methods can be roughly divided into average-based methods [12], [13] and identification-based methods [14], [15]. In the average-based methods, each candidate label has the same probability to be the ground-truth label. They are easy to implement but may be affected by false positive labels. To this end, researchers propose the identification-based methods that treat the ground-truth label as a latent variable and maximize its estimated probability by the maximum margin criterion [16], [17] or maximum likelihood criterion

[8], [18]. Due to their promising results, identification-based methods have attracted increasing attention recently.

Existing PLL methods rely on a fundamental assumption that the ground-truth label must reside in the candidate set. However, this assumption may not be satisfied in real-world scenarios [19], [20]. Figure 1 shows some typical examples. In online object annotation (see Figure 1(a)), different annotators assign distinct labels to the same image. However, due to the complexity of the images and unprofessional judgment of the annotators, the ground-truth label may not be in the candidate set. Another typical application is automatic face naming (see Figure 1(b)). The image with faces is often associated with the text caption, by which we can roughly know who is in the image. However, it is difficult to guarantee that all faces have corresponding names in the text caption. Therefore, we relax the assumption of PLL and focus on a more general problem, noisy PLL, where the ground-truth label may not exist in the candidate set. Due to its intractability, few works have studied this problem.

In this paper, we propose a novel framework for noisy PLL called “Automatic Refinement Network (ARNet)”. It is a multi-round model consisting of two key modules, i.e., noisy sample detection and label correction. Specifically, we first detect noisy samples in the entire dataset. After that, we predict the ground-truth label for each noisy sample and move the predicted label into its candidate set. To guarantee the performance of these modules, we start with warm-up training and automatically determine the correction epoch. Meanwhile, we exploit data augmentation to further reduce prediction errors. We also conduct theoretical analysis and prove the feasibility of ARNet. Through quantitative and qualitative analysis, we demonstrate that our method is able to reduce the noise level of the dataset and outperforms currently advanced approaches in noisy PLL. The main contribution of this paper can be summarized as follows:

- Zheng Lian, Lan Chen and Bin Liu are with National Laboratory of Pattern Recognition, Institute of Automation, Chinese Academy of Sciences, Beijing, China, 100190. E-mail: lian Zheng2016@ia.ac.cn; chen-lan2016@ia.ac.cn; liubin@nlpr.ia.ac.cn.
- Licai Sun is with the School of Artificial Intelligence, University of Chinese Academy of Sciences, Beijing, China, 100049. E-mail: sunlicai2019@ia.ac.cn.
- Jianhua Tao is with National Laboratory of Pattern Recognition, Institute of Automation, Chinese Academy of Sciences, Beijing, China, 100190, with the School of Artificial Intelligence, University of Chinese Academy of Sciences, Beijing, China, 100049 and also with CAS center for Excellence in Brain Science and Intelligence Technology, Beijing, China, 100190. E-mail: jhtao@nlpr.ia.ac.cn.

Manuscript received xxxxxxxx; revised xxxxxxxx. (Corresponding author: Jianhua Tao, Bin Liu)

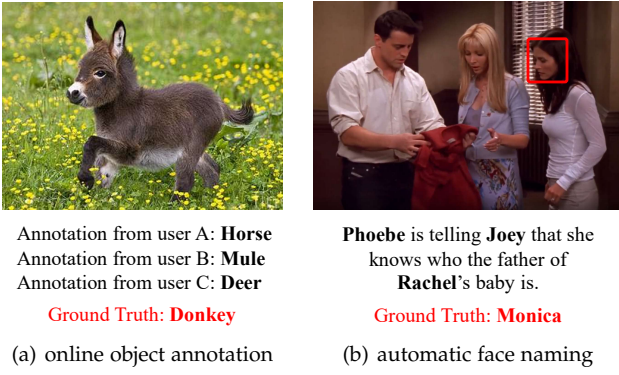


Fig. 1. Typical applications of noisy partial label learning. (a) Candidate labels can be provided by crowdsourcing. However, the ground-truth label may not be in the candidate set due to unprofessional judgments of annotators. (b) Candidate names can be extracted from the text caption. However, there are general cases of faces without names.

- Unlike most existing PLL methods where the ground-truth label must reside in the candidate set, we focus on a seldomly discussed but very important problem, noisy PLL, filling the gap of current works.
- We design a novel framework, ARNet, to deal with noisy PLL. Through theoretical analysis, we demonstrate the feasibility of our proposed method.
- Experimental results on benchmark datasets verify the effectiveness of our method. ARNet is superior to existing state-of-the-art approaches in noisy PLL.

The remainder of this paper is organized as follows: In Section 2, we briefly review some recent works on PLL. In Section 3, we propose a novel framework for noisy PLL with theoretical guarantees. In Section 4, we introduce our experimental datasets, comparison systems and implementation details. In Section 5, we conduct experiments to demonstrate the effectiveness of our method. Finally, we conclude this paper and discuss future work in Section 6.

2 RELATED WORKS

2.1 Non-deep Partial Label Learning

The key challenge of PLL lies in that the ground-truth label of each sample is concealed in the candidate set, but invisible to the learning algorithm. To disambiguate candidate labels, many non-deep PLL methods have been proposed in the past few decades. We roughly divide them into average-based methods and identification-based methods.

Average-based methods assume that each candidate label has the equal probability to be the ground-truth label. For parametric models, Cour et al. [12], [21] proposed to distinguish the average output of candidate labels and non-candidate labels. For instance-based models, Hullermeier et al. [13] estimated the ground-truth label of each sample by voting on the label information of its neighborhood. However, these average-based methods can be severely affected by false positive labels in the candidate set.

Identification-based methods address the shortcoming of average-based methods by directly identifying the ground-truth label and maximizing its estimated probabilities. To implement these methods, researchers have

exploited various techniques, such as maximum margin criterion [16], [17] and maximum likelihood criterion [8], [18]. For example, based on the maximum margin criterion, Nguyen et al. [16] maximized the margin between the maximum output of candidate labels and non-candidate labels. However, it cannot distinguish the ground-truth label from other candidate labels. To this end, Yu et al. [17] directly maximized the margin between the ground-truth label and all other labels. Different from the maximum margin criterion, Jin et al. [18] iteratively optimized the latent ground-truth label and trainable parameters via the maximum likelihood criterion. Considering the fact that different samples and distinct candidate labels contribute differently in the learning process, Tang et al. [22] further utilized the weight of samples and the confidence of candidate labels to facilitate disambiguation. Meanwhile, Liu et al. [8] maximized a mixture-based likelihood function to deal with the PLL problem. In addition, Zhang et al. [23], [24] and Gong et al. [25] leveraged the smoothness assumption (i.e., samples that are close in feature space tend to share the same label) to estimate the confidence of candidate labels. But limited by linear models, these non-deep PLL methods are usually optimized in an inefficient manner.

2.2 Deep Partial Label Learning

In recent years, deep learning has greatly promoted the development of PLL. To implement deep PLL methods, researchers have proposed various training objectives compatible with stochastic optimization. For example, Lv et al. [26] introduced a self-training strategy that exploited model outputs to disambiguate candidate labels. Feng et al. [27] assumed that all incorrect labels had a uniform probability to be candidate labels. Based on this assumption, they further proposed a classifier-consistent algorithm and a risk-consistent algorithm with theoretical guarantees. Wen et al. [28] relaxed the uniform generation assumption in [27]. They introduced a family of loss functions that considered the trade-off between losses on candidate labels and non-candidate labels. Furthermore, Wang et al. [29] proposed PiCO, a PLL method based on contrastive learning. It utilized a prototype-based algorithm to identify the ground-truth label from the candidate set, achieving promising results on multiple benchmark datasets.

The above methods are based on a fundamental assumption that the ground-truth label of each sample must always reside in the candidate set. But due to the unprofessional judgment of the annotators, this assumption may not be satisfied in real-world scenarios.

2.3 Noisy Partial Label Learning

Very recently, some researchers have noticed a more general problem, noisy PLL. Different from traditional PLL, it needs to consider the scenario where the ground-truth label is not in the candidate set. Learning with noisy samples is challenging, and existing approaches cannot directly deal with noisy PLL. Therefore, some new methods have been proposed. Typically, Lv et al. [20] utilized the noise-tolerant loss functions to avoid overemphasizing noise samples in the gradient update. But we find that these methods cannot fully exploit the useful information in noisy samples, thus

TABLE 1
Summary of major mathematical notations.

Notations	Mathematical Meanings
\mathcal{X}, \mathcal{Y}	feature and label space
N, C	number of samples and labels
$\mathcal{D}_S, \tilde{\mathcal{D}}_S$	partially and fully labeled datasets
$\tilde{\mathcal{D}}_S^c, \tilde{\mathcal{D}}_S^n$	clean subset and noisy subset of $\tilde{\mathcal{D}}_S$
q, η	ambiguity level and noise level
x, y, \bar{y}	feature, ground-truth label and incorrect label
$y_j(x)$	the j^{th} element of one-hot encoded label of x
$S(\cdot)$	mapping function from x to its candidate set
ω_1, ω_2	indicator for clean and noisy samples
τ, τ_ϵ	feature and boundary for noisy sample detection
ϕ_c, ϕ_n	hit accuracy for $\tilde{\mathcal{D}}_S^c$ and $\tilde{\mathcal{D}}_S^n$
E_{\max}	maximum number of epochs
e_0	epoch to start correction
$\mathcal{A}(x), K$	$\mathcal{A}(x)$ contains K augmented samples on x
$h(x), h^*(x)$	any classify and Bayes optimal classifier
$p(y = j x)$	posterior probability of x on the label j
y^x	label with the highest posterior probability of x
o^x	label with the second highest posterior probability
$f_j(x)$	estimated probability of x on the label j
$u(x), d(u)$	confidence of x and its density function
c_*, c^*, l	lower bound, upper bound and ratio of $d(u)$
$L(m)$	pure level set with the boundary m
α, ϵ	two values that control the approximate gap
$\lambda_c, \lambda_r, \lambda_g$	hyper-parameters for noise-robust loss functions

limiting their classification performance. To learn a more discriminative classifier, we propose a novel framework to purify noisy samples and reduce the noise level of the dataset. Ideally, we can convert the noisy PLL problem into the traditional PLL problem if all noisy samples are purified.

3 METHODOLOGY

In this section, we first formalize the problem statement for noisy PLL. Then we discuss the motivation and introduce our proposed framework in detail.

3.1 Problem Definition

Let \mathcal{X} be the input space and $\mathcal{Y} = \{1, 2, \dots, C\}$ be the label space. We consider a partially labeled dataset $\mathcal{D}_S = \{(x_i, S(x_i))\}_{i=1}^N$ where the function $S(\cdot)$ maps each sample $x \in \mathcal{X}$ into its corresponding candidate set $S(x) \subseteq \mathcal{Y}$. PLL aims to learn a multi-class classifier $f : \mathcal{X} \rightarrow \mathcal{Y}$ that minimizes the classification risk on \mathcal{D}_S . The basic assumption of PLL is the ground-truth label y must reside in the candidate set $S(x)$. But this assumption may not hold due to the unprofessional judgment of the annotators. Therefore, we focus on a more general problem in this paper, noisy PLL.

We first introduce some necessary notations. The sample x satisfying $y \in S(x)$ is denoted as the *clean* sample, otherwise as the *noisy* sample. We adopt the same generating procedure as previous works to synthesize partially labeled samples [26], [28]. For each sample, any incorrect label $\bar{y} \in \mathcal{Y} \setminus \{y\}$ has a probability q to become an element in the candidate set. After that, each sample has a probability η that y is not concealed in $S(x)$, i.e., $P(y \notin S(x)) = \eta$. We further assume that the label space is known and fixed. Both

clean and noisy samples have their ground-truth labels in this space. The case where x may be an out-of-distribution sample (i.e., $y \notin \mathcal{Y}$) is left for our future work [30], [31].

3.2 Observation and Motivation

The key challenge in noisy PLL is how to deal with noisy samples. For each noisy sample, its ground-truth label y is concealed in the non-candidate set $\{j|j \in \mathcal{Y}, j \notin S(x)\}$. A heuristic solution is to purify the noisy sample by moving y from the non-candidate set into $S(x)$. To this end, we need to realize two core functions: (1) detect noisy samples in the entire dataset; (2) identify the ground-truth label of each noisy sample for label correction. In this section, we conduct pilot experiments on CIFAR-10 ($q = 0.3, \eta = 0.3$) [32] and discuss our motivation in detail.

In the pilot experiments, we consider a fully-labeled dataset $\tilde{\mathcal{D}}_S = \{(x_i, y_i, S(x_i))\}_{i=1}^N$, where the ground-truth label y_i is provided for each sample x_i . Suppose $\omega(x_i) \in \{\omega_1, \omega_2\}$ indicates whether the sample x_i is clean or not:

$$\omega(x_i) = \begin{cases} \omega_1, y_i \in S(x_i) \\ \omega_2, y_i \notin S(x_i). \end{cases} \quad (1)$$

Based on $\omega(x_i)$, we split the dataset $\tilde{\mathcal{D}}_S$ into the clean subset $\tilde{\mathcal{D}}_S^c$ and the noisy subset $\tilde{\mathcal{D}}_S^n$. Here, $|\tilde{\mathcal{D}}_S^c|$ and $|\tilde{\mathcal{D}}_S^n|$ denote the number of samples in these subsets:

$$\tilde{\mathcal{D}}_S^c = \{(x_i, y_i, S(x_i)) | \omega(x_i) = \omega_1, 1 \leq i \leq N\}, \quad (2)$$

$$\tilde{\mathcal{D}}_S^n = \{(x_i, y_i, S(x_i)) | \omega(x_i) = \omega_2, 1 \leq i \leq N\}. \quad (3)$$

3.2.1 Noisy Sample Detection

In noisy PLL, clean samples generally contribute more than noisy samples for better performance. Therefore, we conjecture any metric that can reflect sample contributions can be used for noisy sample detection. In this paper, we focus on the predictive difference between the maximum output of candidate and non-candidate labels [17], a popular metric reflecting sample contributions in traditional PLL [22]. The calculation formula is shown as follows:

$$\tau = \max_{j \in S(x)} f_j(x) - \max_{j \notin S(x)} f_j(x), \quad (4)$$

where $f_j(x)$ represents the estimated probability of the sample x on the label j . Here, $\sum_{j=1}^C f_j(x) = 1$.

In the pilot experiment, we attempt to verify the performance of the feature τ on noisy sample detection. This value depends on the estimate probabilities and therefore changes every epoch. To evaluate its performance, we need to train additional detectors at each epoch, which is time-consuming and computationally expensive. For convenience, we use Bayes error rate $P(\text{error})$ [33]. It is easy to implement and does not require additional training process:

$$P(\text{error}|\tau) = \begin{cases} P(\omega_2|\tau), P(\omega_1|\tau) > P(\omega_2|\tau) \\ P(\omega_1|\tau), P(\omega_1|\tau) < P(\omega_2|\tau), \end{cases} \quad (5)$$

$$\begin{aligned} P(\text{error}) &= \int P(\text{error}|\tau) p(\tau) d\tau \\ &= \int_{\mathcal{R}_1} P(\omega_2|\tau) p(\tau) d\tau + \int_{\mathcal{R}_2} P(\omega_1|\tau) p(\tau) d\tau \\ &= \int_{\mathcal{R}_1} p(\tau|\omega_2) P(\omega_2) d\tau + \int_{\mathcal{R}_2} p(\tau|\omega_1) P(\omega_1) d\tau. \end{aligned} \quad (6)$$

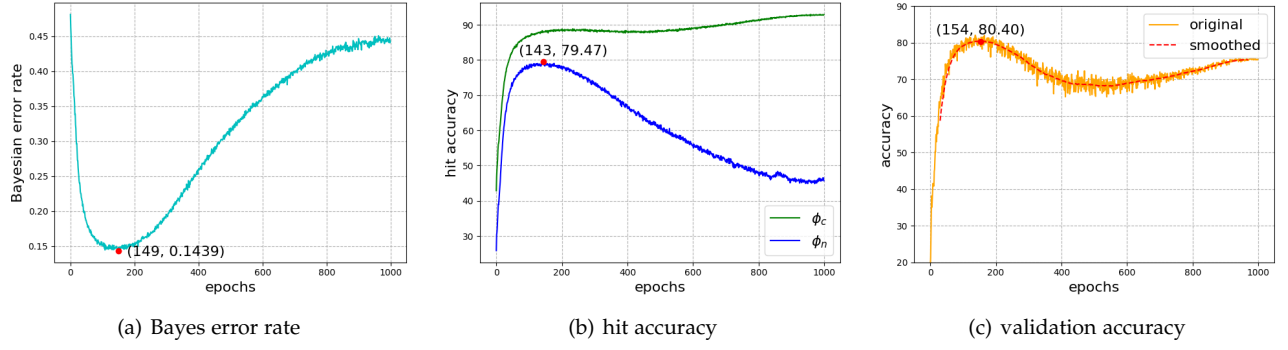


Fig. 2. Visualization Bayes error rate, hit accuracy and validation accuracy on CIFAR-10 ($q = 0.3, \eta = 0.3$). We mark the minima in (a), the maxima in (b) and the local maxima in (c) with red dots.

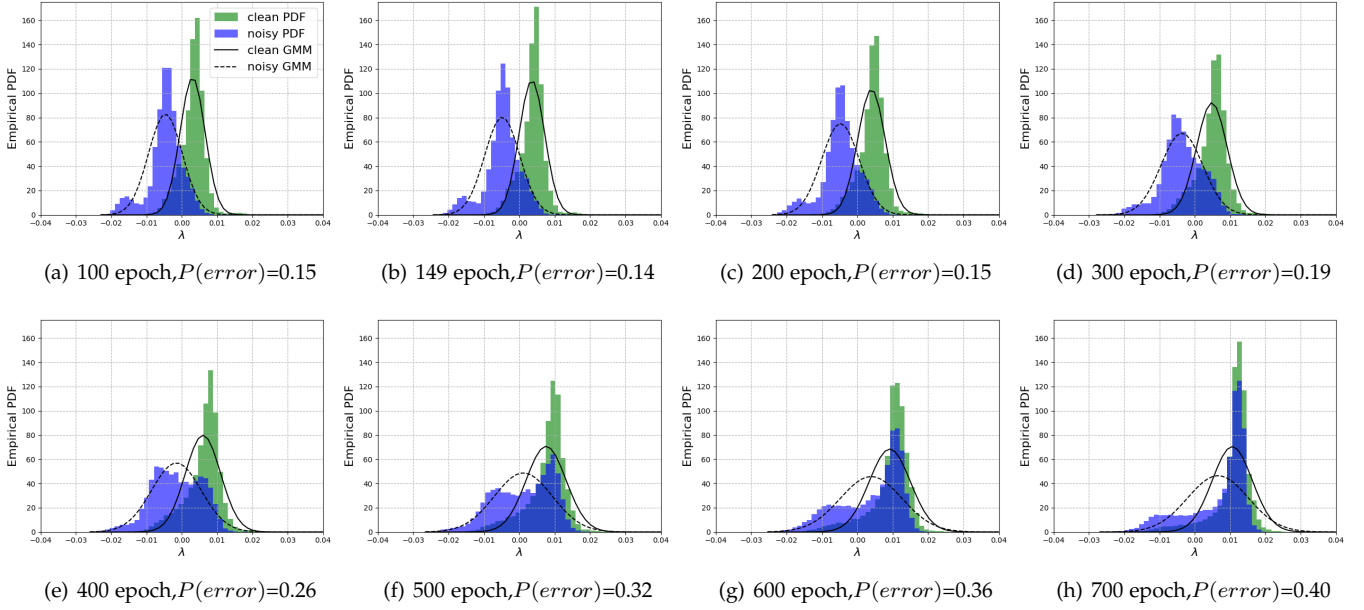


Fig. 3. Empirical PDF and estimated GMM models on CIFAR-10 ($q = 0.3, \eta = 0.3$) with increasing training iterations.

Based on whether satisfying $P(\omega_1|\tau) > P(\omega_2|\tau)$, we divide the space into two regions \mathcal{R}_1 and \mathcal{R}_2 . Here, $P(\omega_1)$ and $P(\omega_2)$ are the prior probabilities to distinguish clean and noisy samples. Since we cannot obtain such priors, we set them to $P(\omega_1) = P(\omega_2) = 0.5$. Meanwhile, we leverage histograms to approximate the class-conditional probability density functions $P(\tau|\omega_1)$ and $P(\tau|\omega_2)$.

Experimental results are shown in Fig. 2(a). Lower Bayes error rate means better performance on noisy sample detection. If we randomly determine whether a sample is clean or noisy, the Bayes error rate is $P(\text{error}) = 0.50$. From Fig. 2(a), we observe that the Bayes error rate can reach $P(\text{error}) = 0.14$, which is much lower than random guessing. Therefore, we can infer from τ whether a sample is more likely to be clean or noisy.

3.2.2 Label Correction

After noisy sample detection, we attempt to identify the ground-truth label for each noisy sample, so that we can correct the noisy sample by moving the ground-truth label into its candidate set.

For the clean sample, previous works generally select the candidate label with the highest probability $\arg \max_{j \in S(x)} f_j(x)$ as the predicted label [22], [34]. For the noisy sample, y is concealed in the non-candidate set. Naturally, we conjecture that the non-candidate label with the highest probability $\arg \max_{j \notin S(x)} f_j(x)$ can be regraded as the predicted label for noisy samples. To verify this assumption, we conduct a pilot experiment. Firstly, we define an evaluation metric called *hit accuracy*:

$$\phi_c = \frac{1}{|\tilde{\mathcal{D}}_S^c|} \sum_{(x,y,S(x)) \in \tilde{\mathcal{D}}_S^c} \mathbb{I} \left(y = \arg \max_{j \in S(x)} f_j(x) \right), \quad (7)$$

$$\phi_n = \frac{1}{|\tilde{\mathcal{D}}_S^n|} \sum_{(x,y,S(x)) \in \tilde{\mathcal{D}}_S^n} \mathbb{I} \left(y = \arg \max_{j \notin S(x)} f_j(x) \right), \quad (8)$$

where $\mathbb{I}(\cdot)$ is the indicator function. ϕ_c is the hit accuracy for the clean subset and ϕ_n is the hit accuracy for the noisy subset. This metric measures the performance of our method

on ground-truth label detection. Higher hit accuracy means better performance.

Experimental results are shown in Fig. 2(b). If we randomly select a non-candidate label as the predicted label for each noisy sample, ϕ_n is calculated as follows:

$$\begin{aligned}\phi_n &= \frac{1}{C - \mathbb{E}_{x \sim \mathcal{D}_S} [|S(x)|]} \\ &= \frac{1}{C - (1 + (C - 1) * q)},\end{aligned}\quad (9)$$

where $\mathbb{E}_{x \sim \mathcal{D}_S} [|S(x)|]$ denotes the expectation on the number of candidate labels. Since we conduct pilot experiments on CIFAR-10 ($q = 0.3, \eta = 0.3$), the hit accuracy of random guessing is $\phi_n = 15.87$. Experimental results in Fig. 2(b) demonstrate that our method can reach $\phi_n = 79.47$, which is much higher than random guessing. These results verify the effectiveness of our approach in identifying ground-truth labels for noisy samples.

3.3 Automatic Refinement Network

Motivated by the above observations, we propose a simple yet effective framework for noisy PLL. Our ARNet consists of two key modules: noisy sample detection and label correction. However, we find the following challenges during implementation: (1) As shown in Fig. 2(a)~2(b), these modules perform poorly at the early epochs of training. Therefore, we need to find an appropriate epoch e_0 . Before e_0 , we start with a warm-up period with traditional PLL approaches. After that, we exploit ARNet for label correction; (2) Different from pilot experiments in Section 3.2, the ground-truth labels are not available in real-world scenarios. Therefore, we need to find appropriate unsupervised techniques to realize these modules. In this section, we present our solutions to the above challenges.

3.3.1 Choice of Correction Epoch

An appropriate e_0 is the epoch when noisy sample detection and label correct can achieve good performance. As shown in Fig. 2(a)~2(b), the performance of these modules first increases and then decreases. Meanwhile, we observe that these modules achieve the best performance at close epochs. To find an appropriate e_0 , we need to reveal the reason behind these phenomena.

Previous works have demonstrated that when there are a mixture of clean and noisy samples, networks tend to fit the former before the latter [35], [36]. Based on this theory, networks first fit clean samples in noisy PLL, resulting in the performance improvement. At the late epochs of training, networks start fitting noisy samples. Since the ground-truth label is not concealed in the candidate set, networks assign wrong predictions on the candidate set and gradually become overconfident during training. This process harms the discriminative performance of τ and leads to the decrement of ϕ_n . Therefore, the epoch when networks start fitting noisy samples is an appropriate e_0 for correction.

Empirically, networks cannot perform accurately on unseen data when fitting noisy samples, resulting in a drop in validation accuracy. Therefore, we conjecture that the validation accuracy can be used to find e_0 . To verify this assumption, we visualize the curve of validation accuracy

in Fig. 2(c). We observe that it first increases and then decreases, the same trend as in Fig. 2(a)~2(b). At the late epochs of training, it gradually increases and converges to a stable value. Since ϕ_c keeps increasing during training (see Fig. 2(b)), the increasement brought by the clean samples is greater than the decrement brought by the noise samples, resulting in a slight improvement in validation accuracy. Therefore, we choose the epoch of the first local maximum as e_0 . Experimental results demonstrate that the epoch chosen by our method (the 154th epoch) is close to the best epoch for noisy sample detection (the 149th epoch) and label correct (the 143th epoch). These results verify the effectiveness of our method.

3.3.2 Noisy Sample Detection

To achieve better performance in noisy PLL, we need to find an appropriate approach for noisy sample detection. Since ground-truth labels are not available in real-world scenarios, we rely on the unsupervised techniques for this purpose.

Previous works [37] generally exploit the Gaussian Mixture Model (GMM) [38], a popular unsupervised modeling technique. To verify its performance, we visualize the empirical PDF and estimated GMM on τ for clean and noisy subsets. From Fig. 3, we observe that the Gaussian is a poor approximation to the distribution. Therefore, we need to find a more effective method to detect noisy samples.

Meanwhile, we observe some interesting phenomena. As the number of training iterations increases, the range of τ is quite fixed and most samples satisfy $\tau \in [-0.3, 0.3]$. Meanwhile, the samples satisfying $\tau < -0.1$ have a high probability to be the noisy samples. Inspired by the above phenomena, we determine the samples satisfying $\tau < -\tau_\epsilon$ as the noisy samples, where τ_ϵ is a user-defined parameter.

3.3.3 Label Correction

After noisy sample detection, we aim to find the ground-truth label of each noisy sample for label correction. In this paper, we use the non-candidate label with the highest probability as the predicted label. However, the prediction results cannot be completely correct. To achieve better performance, we need to further reduce errors in this module.

A straightforward solution is to encourage the model's output not to be significantly affected by natural and small input changes. Such process improves the robustness of the model and increases the reliability of the prediction. Specifically, we assume that each sample has a set of random augmented samples $\mathcal{A}(x) = \{\text{Aug}_k(x) | 1 \leq k \leq K\}$, where K denotes the number of augmentations and $\text{Aug}_k(x)$ denotes the k^{th} augmented version. In ARNet, we select samples that satisfy the following conditions for label correction:

$$\max_{j \in S(x)} f_j(x) - \max_{j \notin S(x)} f_j(x) < -\tau_\epsilon, \quad (10)$$

$$\max_{j \in S(x)} f_j(z) - \max_{j \notin S(x)} f_j(z) < -\tau_\epsilon, \forall z \in \mathcal{A}(x), \quad (11)$$

$$\arg \max_{j \in S(x)} f_j(x) = \arg \max_{j \in S(x)} f_j(z), \forall z \in \mathcal{A}(x). \quad (12)$$

Overall, we rely on stricter criteria for noisy sample detection and label correction. Besides the original samples, their augmented versions should meet additional conditions. We find that such process can reduce errors in these

modules and improve the performance on noisy PLL. The pseudo-code of ARNet is summarized in Algorithm 1.

3.4 Theoretical Analysis

Inspired by previous works [39], [40], we further conduct theoretical analysis to demonstrate the feasibility of ARNet. For convenience, we first introduce some necessary notations. The goal of supervised learning and noisy PLL is to learn a classifier that can make correct predictions on unseen data. We usually take the highest estimated probability as the predicted label $h(x) = \arg \max_{j \in \mathcal{Y}} f_j(x)$. We assume that all possible $h(x)$ form the hypothesis space \mathcal{H} .

In supervised learning, each sample has a ground-truth label, i.e., $\mathcal{D} = \{(x_i, y_i)\}_{i=1}^N$. The Bayes optimal classifier $h^*(x)$ is the one that minimizes the following risk:

$$h^*(x) = \arg \min_{h \in \mathcal{H}} \mathbb{E}_{(x,y) \sim \mathcal{D}} \mathbb{I}(h(x) \neq y). \quad (13)$$

Different from supervised learning, each sample is associated with a set of candidate labels in noisy PLL, i.e., $\mathcal{D}_S = \{(x_i, S(x_i))\}_{i=1}^N$. The optimal classifier $f(x)$ is the one that can minimize the risk under a suitable PLL loss \mathcal{L} :

$$f(x) = \arg \min_{f \in \mathcal{H}} \mathbb{E}_{(x,S(x)) \sim \mathcal{D}_S} \mathcal{L}(f(x), S(x)). \quad (14)$$

We assume that \mathcal{H} is sufficiently complex, so that $f(x)$ can approximate the Bayes optimal classifier $h^*(x)$. Let y^x (or o^x) be the label with the highest (or second highest) posterior possibility, i.e., $y^x = \arg \max_{j \in \mathcal{Y}} p(y = j|x)$, $o^x = \arg \max_{j \in \mathcal{Y}, j \neq y^x} p(y = j|x)$. We measure the confidence of x by the margin $u(x) = p(y^x|x) - p(o^x|x)$.

Definition 1 (Pure (m, f, S) -level set). A set $L(m) = \{x|u(x) \geq m\}$ is pure for (f, S) if all $x \in L(m)$ satisfy: (1) $y^x \in S(x)$; (2) $y^x = \arg \max_{j \in \mathcal{Y}} f_j(x)$.

Assumption 1 (Level set (α, ϵ) consistency). Let $I(x, z)$ be the indicator function for two samples x and z . It is equal to 1 if the more confident sample z satisfies $y^z \notin S(z)$, i.e., $I(x, z) = \mathbb{I}[y^z \notin S(z)|u(z) \geq u(x)]$. Suppose there exist two constants $\alpha > 0, 0 < \epsilon < 1$ and $S_{init}(x)$ is the initial candidate set of x . For any mapping function $S(\cdot)$ satisfying $|S(x)| = |S_{init}(x)|$, all $x \in \mathcal{D}_S$ should meet the condition:

$$|f_j(x) - p(y = j|x)| < \alpha \mathbb{E}_{(z,S(z)) \sim \mathcal{D}_S} [I(x, z)] + \frac{\epsilon}{6}.$$

The approximation error between $f_j(x)$ and $p(y = j|x)$ is controlled by the noise level of the dataset. Particularly, if y^x is concealed in $S(x)$ for all $x \in \mathcal{D}_S$, we will obtain a tighter constraint $|f_j(x) - p(y = j|x)| < \frac{\epsilon}{6}$.

Assumption 2 (Level set bounded distribution). Let $d(u)$ be the density function of $u(x)$. Suppose there exist two constants $0 < c_* < c^*$ such that the density function $d(u)$ is bounded by $c_* < d(u) < c^*$. We denote the imbalance ratio as $l = c^*/c_*$.

This assumption enforces the continuity of $d(u)$. It is crucial in analysis since it allows borrowing information from the neighborhood to help correct noisy samples. If Assumption 1~2 hold, we can prove the following theorems:

Theorem 1 (One-round refinement). Assume that there exists a boundary $\epsilon < m < 1$ such that $L(m)$ is pure for (f, S) . For all $x \in \mathcal{D}_S$ satisfying $\max_{j \notin S(x)} f_j(x) - \max_{j \in S(x)} f_j(x) \geq$

$m_{new} - \epsilon$, we move $\arg \max_{j \notin S(x)} f_j(x)$ into $S(x)$ and move $\arg \min_{j \in S(x)} f_j(x)$ out of $S(x)$, thus generating the updated candidate set $S_{new}(x)$. After that, we train a new classifier $f^{new}(x)$ on the updated dataset $\mathcal{D}_{S_{new}} = \{(x_i, S_{new}(x_i))\}_{i=1}^N$:

$$f^{new}(x) = \arg \min_{h \in \mathcal{H}} \mathbb{E}_{(x,S_{new}(x)) \sim \mathcal{D}_{S_{new}}} \mathcal{L}(h(x), S_{new}(x)).$$

$L(m_{new})$ is pure for (f^{new}, S_{new}) when m_{new} satisfies:

$$(1 + \frac{\epsilon}{6\alpha l})(1 - m) \leq 1 - m_{new} \leq (1 + \frac{\epsilon}{3\alpha l})(1 - m).$$

Theorem 2 (Multi-round refinement). For an initial dataset satisfying $P(y^x \notin S_{init}(x)) = \eta$, we assume that there exists a boundary $\max(2\alpha\eta + \epsilon/3, \epsilon) < m_{init} < 1$ such that $L(m_{init})$ is pure for (f^{init}, S_{init}) . Repeat the one-round refinement in Theorem 1. After $R > \frac{6l\alpha}{\epsilon} \log(\frac{1-\epsilon}{1-m_{init}})$ rounds with $m_{end} = \epsilon$, we obtain the final candidate set and classifier (S_{final}, f^{final}) that satisfy:

$$P(y^x \notin S_{final}(x)) \leq c^* \epsilon,$$

$$P\left(\arg \max_{j \in \mathcal{Y}} f_j^{final}(x) = h^*(x)\right) \geq 1 - c^* \epsilon.$$

The above theorems demonstrate that our multi-round ARNet is able to reduce the noise level of the dataset and eventually approximate the Bayes optimal classifier. The detailed proof can be found in Appendix.

4 EXPERIMENTAL DATABASES AND SETUP

In this section, we first describe the benchmark datasets in our experiments. Following that, we introduce various currently advanced baselines for comparison. Finally, we provide a detailed illustration about our implementation.

4.1 Corpus Description

We conduct experiments on four benchmark datasets for PLL, including CIFAR-10 [32], CIFAR-100 [32], MNIST [41] and Kuzushiji-MNIST [42]. We manually corrupt these datasets into noisy partially labeled versions. To form the candidate set for clean samples, we flip incorrect labels to false positive labels with a probability q and aggregate the flipped ones with the ground-truth label, in line with previous works [26], [28]. After that, each sample has a probability η to become a noisy sample. To form the candidate set for noisy samples, we further select a negative label from the non-candidate set, move it into the candidate set, and move the ground-truth label out of the candidate set.

In this paper, we denote the probability q as the ambiguity level and the probability η as the noise level. The ambiguity level controls the number of candidate labels and the noise level controls the percentage of noisy samples. Since CIFAR-100 has more labels than other datasets, we consider $q \in \{0.01, 0.03, 0.05\}$ for CIFAR-100 and $q \in \{0.1, 0.3, 0.5\}$ for others. On MNIST, all methods can achieve high accuracy at low noise levels. To show the advantage of our method, we choose more challenging conditions for this dataset. Specifically, we consider $\eta \in \{0.2, 0.3, 0.4\}$ for MNIST and $\eta \in \{0.1, 0.2, 0.3\}$ for others.

4.2 Baselines

In this section, we conduct comparative experiments with currently advanced PLL methods and noisy PLL methods.

Algorithm 1: ARNet Algorithm

Input: PLL training set $\mathcal{D}_S = \{(x_i, S(x_i))\}_{i=1}^N$, the predictive model f , the margin τ_ϵ , the number of augmentations K , the number of epochs E_{\max} , the number of iteration T_{\max} .

Output: The optimized model f .

```

1 Initialize model parameters for  $f$ ;
2 for  $e = 1, \dots, E_{\max}$  do
3   Shuffle  $\mathcal{D}_S$ ;
4   for  $t = 1, \dots, T_{\max}$  do
5     Sample mini-batch  $\mathcal{B}_t = \{(x_i, S(x_i))\}_{i=1}^{N_t}$ ;
6     Train the predictive model  $f$  on  $\mathcal{B}_t$ ;
7   end
8   Evaluate  $f$  using validation accuracy and save the result in  $res^{[e]}$ ;
9   if  $e \geq 10$  then
10    Check the convergence condition  $\sum_{i=e-9}^e (res^{[i]} - res^{[i-1]}) < 10^{-5}$ ;
11    if converged then
12       $e_0 = e$ ;
13      break;
14    end
15  end
16 end
17
18 for  $e = e_0, \dots, E_{\max}$  do
19   Shuffle  $\mathcal{D}_S$ ;
20   for  $t = 1, \dots, T_{\max}$  do
21     Sample mini-batch  $\mathcal{B}_t = \{(x_i, S(x_i))\}_{i=1}^{N_t}$ ;
22     Train the predictive model  $f$  on  $\mathcal{B}_t$ ;
23     if  $i = 1, \dots, N_t$  then
24       if  $x_i$  satisfies the conditions in Eq. 10~12 then
25         Identify  $x_i$  as the noisy sample;
26         Gain the predicted label  $\arg \max_{j \notin S(x_i)} f_j(x_i)$  for  $x_i$ ;
27         Correct the noisy sample  $x_i$  by moving the predicted label into its candidate set  $S(x_i)$ ;
28       end
29     end
30   end
31 end

```

4.2.1 PLL Methods

To evaluate the performance of our ARNet, we implement the following state-of-the-art PLL methods as baselines:

CC [27] is a classifier-consistent method that leverages the cross entropy loss function and the transition matrix to form an empirical risk estimator.

RC [27] is a risk-consistent method that exploits the importance re-weighting strategy to approximate the optimal classifier. Its algorithm process is consistent with PRODEN [26], but with additional theoretical guarantees.

LOG [43] is a strong benchmark model. It exploits an upper-bound loss to improve the classification performance.

LWC [28] is a leveraged weighted (LW) loss that considers the trade-off between losses on candidate labels and non-candidate labels. In this model, we employ the cross entropy loss function for LW.

LWS [28] is a variant of LWC. Different from LWC, we employ the sigmoid loss function for LW.

PiCO [29] is based on contrastive learning. It exploits a prototype-based algorithm to identify the ground-truth

label from the candidate set. This model outperforms other baselines under varying ambiguity levels [29].

4.2.2 Noisy PLL Methods

ARNet corrects the noisy sample by moving its ground-truth label from the non-candidate set into the candidate set. Unlike ARNet, existing noisy PLL methods rely on noise-robust loss functions and do not leverage label correction [20]. To introduce these loss functions clearly, we convert the ground-truth label into its one-hot version $y_j(x), j \in [1, C]$. Here, $y_j(x) = 1$ if $j = y$, otherwise 0.

Mean Absolute Error (MAE) is bounded and symmetric. Previous works have demonstrated that this loss function is robust to label noise [44]:

$$\mathcal{L}_{\text{MAE}} = - \sum_{j=1}^C \|y_j(x) - f_j(x)\|_1. \quad (15)$$

Mean Square Error (MSE) is bounded but not symmet-

ric. Same with MAE, it is robust to label noise [44]:

$$\mathcal{L}_{\text{MSE}} = - \sum_{j=1}^C \|y_j(x) - f_j(x)\|_2^2. \quad (16)$$

Symmetric Cross Entropy (SCE) combines Reverse Cross Entropy (RCE) with Categorical Cross Entropy (CCE) via two hyper-parameters λ_c and λ_r [45]. This loss function exploits the benefits of the noise-robustness provided by RCE and the implicit weighting scheme of CCE:

$$\mathcal{L}_{\text{CCE}} = - \sum_{j=1}^C y_j(x) \log f_j(x), \quad (17)$$

$$\mathcal{L}_{\text{RCE}} = - \sum_{j=1}^C f_j(x) \log y_j(x), \quad (18)$$

$$\mathcal{L}_{\text{SCE}} = \lambda_c \mathcal{L}_{\text{CCE}} + \lambda_r \mathcal{L}_{\text{RCE}}. \quad (19)$$

Generalized Cross Entropy (GCE) [46] adopts the negative Box-Cox transformation and uses a hyper-parameter λ_g to balance MAE and CCE:

$$\mathcal{L}_{\text{GCE}} = - \sum_{j=1}^C y_j(x) \left(\frac{1 - f_j(x)^{\lambda_g}}{\lambda_g} \right). \quad (20)$$

4.3 Implementation Details

In this paper, we propose an effective and flexible ARNet that can be integrated with existing PLL methods. Since PiCO [29] has demonstrated its performance in PLL, we integrate ARNet with PiCO for noisy PLL. There are two user-specific parameters in ARNet, i.e., the margin τ_ϵ and the number of augmentations K . We select τ_ϵ from $\{0.0001, 0.001, 0.002, 0.004, 0.008, 0.016\}$ and K from $\{1, 2\}$. To optimize all trainable parameters, we leverage the SGD optimizer and set the number of epochs to $E_{\max} = 1000$. We choose an initial learning rate from $\{0.001, 0.01\}$ and adjust it using the cosine scheduler. To evaluate the performance of different methods, we run each experiment three times with different random seeds and report the average results on the test set. All experiments are implemented with PyTorch [47] and carried out with NVIDIA Tesla V100 GPU.

For PLL baselines, we use the identical experimental settings according to the original methods for a fair comparison. For noisy PLL baselines, we rely on noise-robust loss functions and do not consider label correction. There are two hyper-parameters in SCE, i.e., λ_c and λ_r . We choose λ_c from $\{0.1, 1.0, 6.0\}$ and λ_r from $\{0.1, 1.0\}$. Meanwhile, we select the user-specific parameter λ_g in GCE from $\{0.5, 0.6, 0.7\}$.

5 RESULTS AND DISCUSSION

In this section, we first compare the inductive and transductive performance with currently advanced approaches under varying ambiguity and noise levels. Then, we show the noise robustness of our method and reveal the impact of augmentation strategies. Next, we conduct parameter sensitivity analysis and study the role of swapping in label correction. Finally, we visualize the latent representations to qualitatively analyze the strengths of our method.

5.1 Inductive Performance

In Table 2~3, we compare the inductive performance with existing PLL methods and noisy PLL methods. Inductive results indicate the classification accuracy in the test set, i.e., test accuracy [26], [48]. Since the standard deviation is small under different settings (see Table 2), we only report the average results in Table 3. From these quantitative results, we have the following observations:

1. Experimental results in Table 2 demonstrate that ARNet succeeds over existing PLL methods on all datasets. Taking the results on CIFAR-10 as an example, ARNet outperforms the currently advanced approaches by 1.91%~17.44%. On CIFAR-100, our method shows an absolute improvement of 2.90%~9.91% over baselines. We also observe similar phenomena on other datasets. The reason lies in that existing PLL methods are mainly designed for clean samples. However, noisy samples may exist due to the unprofessional judgment of annotators. To this end, we propose ARNet that can correct noisy samples by moving the ground-truth label into the candidate set. These results verify the effectiveness of our method under noisy conditions.

2. From Table 2, we observe that the advantage of our method becomes more significant with increasing noise levels. Taking the results on CIFAR-10 ($q = 0.3$) as an example, the performance gap increases from 2.39% to 9.10% as the noise level increases from 0.1 to 0.3. Meanwhile, the performance degradation of our method is much smaller than that of baselines. Taking the results on CIFAR-10 ($q = 0.3$) as an example, as the noise level increases from 0.1 to 0.3, the performance of baselines drops by 6.01%~11.23% while ARNet only drops by 0.75%. These results demonstrate the noise robustness of our method.

3. Compared with existing noisy PLL methods, we observe that our ARNet also achieves better performance than these baselines (see Table 3). They mainly utilize the noise-tolerant loss functions to avoid overemphasizing noise samples in the gradient update. However, they are unable to fully exploit the useful information in these samples. Differently, our ARNet can progressively purify noisy samples to clean ones, allowing us to leverage plenty of clean samples to learn more a discriminative classifier.

5.2 Transductive Performance

Besides the inductive performance, we also evaluate the transductive performance of different methods. Transductive results reflect the disambiguation ability on the training set [26], [48]. In traditional PLL, the basic assumption is that the ground-truth label of each sample must reside in the candidate set. To evaluate the transductive performance, previous works [49] determine the ground-truth label of each sample as $\arg \max_{j \in S(x)} f_j(x)$. But this assumption does not hold in noisy PLL. Therefore, we determine the ground-truth label from the entire label space rather than the candidate set, i.e., $\arg \max_{j \in \mathcal{Y}} f_j(x)$.

Experimental results are shown in Fig. 4. From this figure, we observe that ARNet consistently outperforms all baselines on all datasets. Existing methods either ignore the presence of noisy samples or fail to exploit them effectively. Compared with existing methods, we leverage the idea of

TABLE 2

Inductive performance (mean \pm std) comparison with various PLL methods. The best performance is highlighted in bold, and the second-highest result is labeled by \dagger . The column with Δ_{SOTA} means the improvements or reductions of ARNet compared to existing methods.

Dataset	q	η	CC	LOG	LWC	LWS	RC	PiCO	ARNet	Δ_{SOTA}
CIFAR-10	0.1	0.1	79.81 \pm 0.22	79.81 \pm 0.23	79.13 \pm 0.53	82.97 \pm 0.24	80.87 \pm 0.30	90.78 \pm 0.24 \dagger	92.69\pm0.16	\uparrow 1.91
		0.2	77.06 \pm 0.18	76.44 \pm 0.50	76.15 \pm 0.46	79.46 \pm 0.09	78.22 \pm 0.23	87.27 \pm 0.11 \dagger	92.12\pm0.09	\uparrow 4.85
		0.3	73.87 \pm 0.31	73.36 \pm 0.56	74.17 \pm 0.48	74.28 \pm 0.79	75.24 \pm 0.17	84.96 \pm 0.12 \dagger	92.04\pm0.21	\uparrow 7.08
	0.3	0.1	74.09 \pm 0.60	73.85 \pm 0.30	77.47 \pm 0.56	80.93 \pm 0.28	79.69 \pm 0.37	89.71 \pm 0.18 \dagger	92.10\pm0.02	\uparrow 2.39
		0.2	71.43 \pm 0.56	71.44 \pm 0.41	74.02 \pm 0.35	76.07 \pm 0.38	75.69 \pm 0.63	85.78 \pm 0.23 \dagger	91.69\pm0.26	\uparrow 5.91
		0.3	68.08 \pm 1.12	67.17 \pm 0.75	69.10 \pm 0.59	69.70 \pm 0.72	71.01 \pm 0.54	82.25 \pm 0.32 \dagger	91.35\pm0.08	\uparrow 9.10
	0.5	0.1	69.87 \pm 0.94	70.33 \pm 0.80	70.59 \pm 1.34	70.41 \pm 2.68	72.46 \pm 1.51	88.11 \pm 0.29 \dagger	91.51\pm0.05	\uparrow 3.40
		0.2	59.35 \pm 0.22	59.81 \pm 0.23	57.42 \pm 1.14	58.26 \pm 0.28	59.72 \pm 0.42	82.41 \pm 0.30 \dagger	90.76\pm0.10	\uparrow 8.35
		0.3	48.93 \pm 0.52	49.64 \pm 0.46	48.93 \pm 0.37	39.42 \pm 3.09	49.74 \pm 0.70	68.75 \pm 2.62 \dagger	86.19\pm0.41	\uparrow 17.44
CIFAR-100	0.01	0.1	53.63 \pm 0.46	53.10 \pm 0.61	53.16 \pm 0.87	56.05 \pm 0.20	52.73 \pm 1.05	68.27 \pm 0.08 \dagger	71.17\pm0.14	\uparrow 2.90
		0.2	48.84 \pm 0.19	48.97 \pm 0.17	48.64 \pm 0.33	50.66 \pm 0.59	48.59 \pm 1.04	62.24 \pm 0.31 \dagger	70.10\pm0.28	\uparrow 7.86
		0.3	45.50 \pm 0.28	45.16 \pm 0.29	45.51 \pm 0.28	45.71 \pm 0.45	45.77 \pm 0.31	58.97 \pm 0.09 \dagger	68.77\pm0.28	\uparrow 9.80
	0.03	0.1	51.85 \pm 0.18	51.85 \pm 0.35	51.69 \pm 0.28	53.59 \pm 0.45	52.15 \pm 0.19	67.38 \pm 0.09 \dagger	71.01\pm0.43	\uparrow 3.63
		0.2	47.48 \pm 0.30	47.82 \pm 0.33	47.60 \pm 0.44	48.28 \pm 0.44	48.25 \pm 0.38	62.01 \pm 0.33 \dagger	70.15\pm0.17	\uparrow 8.14
		0.3	43.37 \pm 0.42	43.43 \pm 0.30	43.39 \pm 0.18	42.20 \pm 0.49	43.92 \pm 0.37	58.64 \pm 0.28 \dagger	68.18\pm0.30	\uparrow 9.54
	0.05	0.1	50.64 \pm 0.40	51.27 \pm 1.22	50.55 \pm 0.34	45.46 \pm 0.44	46.62 \pm 0.34	67.52 \pm 0.43 \dagger	70.73\pm0.09	\uparrow 3.21
		0.2	45.87 \pm 0.36	45.88 \pm 0.13	45.85 \pm 0.28	39.63 \pm 0.80	45.46 \pm 0.21	61.52 \pm 0.28 \dagger	69.33\pm0.51	\uparrow 7.81
		0.3	40.84 \pm 0.47	41.20 \pm 0.60	39.83 \pm 0.30	33.60 \pm 0.64	40.31 \pm 0.55	58.18 \pm 0.65 \dagger	68.09\pm0.12	\uparrow 9.91
MNIST	0.1	0.2	96.84 \pm 0.07	96.77 \pm 0.11	96.77 \pm 0.13	97.48 \pm 0.10	97.03 \pm 0.08	99.17 \pm 0.10 \dagger	99.26\pm0.01	\uparrow 0.09
		0.3	96.20 \pm 0.14	96.19 \pm 0.11	96.23 \pm 0.20	96.75 \pm 0.09	96.51 \pm 0.20	99.00 \pm 0.07 \dagger	99.23\pm0.03	\uparrow 0.23
		0.4	95.30 \pm 0.16	95.22 \pm 0.21	95.34 \pm 0.12	95.77 \pm 0.13	95.65 \pm 0.21	99.00 \pm 0.04 \dagger	99.21\pm0.01	\uparrow 0.21
	0.3	0.2	95.83 \pm 0.25	95.75 \pm 0.16	96.08 \pm 0.22	96.86 \pm 0.07	96.42 \pm 0.13	99.07 \pm 0.07 \dagger	99.24\pm0.03	\uparrow 0.17
		0.3	94.33 \pm 0.22	94.53 \pm 0.16	94.75 \pm 0.18	95.52 \pm 0.09	95.30 \pm 0.09	98.92 \pm 0.02 \dagger	99.23\pm0.03	\uparrow 0.31
		0.4	91.96 \pm 0.31	92.01 \pm 0.28	92.49 \pm 0.12	93.54 \pm 0.22	93.29 \pm 0.22	98.69 \pm 0.06 \dagger	99.16\pm0.04	\uparrow 0.47
	0.5	0.2	93.54 \pm 0.27	93.41 \pm 0.15	94.25 \pm 0.21	95.82 \pm 0.11	95.03 \pm 0.09	98.93 \pm 0.03 \dagger	99.18\pm0.07	\uparrow 0.25
		0.3	89.43 \pm 0.45	89.54 \pm 0.23	89.69 \pm 0.48	91.38 \pm 0.35	91.59 \pm 0.47	98.70 \pm 0.05 \dagger	99.12\pm0.02	\uparrow 0.42
		0.4	74.97 \pm 0.74	74.30 \pm 1.89	71.03 \pm 1.73	52.19 \pm 3.31	78.51 \pm 0.95 \dagger	76.39 \pm 1.10	98.17\pm1.27	\uparrow 19.66
Kuzushiji-MNIST	0.1	0.1	88.43 \pm 0.28	88.09 \pm 0.17	88.12 \pm 0.22	89.80 \pm 0.25	88.83 \pm 0.17	97.55 \pm 0.04 \dagger	98.07\pm0.07	\uparrow 0.52
		0.2	86.22 \pm 0.27	86.08 \pm 0.31	86.13 \pm 0.46	87.32 \pm 0.44	86.76 \pm 0.36	96.95 \pm 0.16 \dagger	97.96\pm0.03	\uparrow 1.01
		0.3	83.82 \pm 0.15	83.60 \pm 0.36	83.82 \pm 0.24	84.79 \pm 0.18	84.31 \pm 0.24	96.53 \pm 0.18 \dagger	97.95\pm0.07	\uparrow 1.42
	0.3	0.1	85.46 \pm 0.45	85.63 \pm 0.35	86.20 \pm 0.23	87.84 \pm 0.26	87.17 \pm 0.32	97.34 \pm 0.05 \dagger	97.97\pm0.03	\uparrow 0.63
		0.2	82.15 \pm 0.70	82.39 \pm 0.61	82.95 \pm 0.53	84.61 \pm 0.57	84.28 \pm 0.42	96.57 \pm 0.06 \dagger	97.96\pm0.09	\uparrow 1.39
		0.3	77.34 \pm 0.65	78.06 \pm 0.49	79.16 \pm 0.42	79.79 \pm 0.65	80.79 \pm 0.49	95.34 \pm 0.34 \dagger	97.87\pm0.10	\uparrow 2.53
	0.5	0.1	81.97 \pm 0.35	81.46 \pm 0.17	82.89 \pm 0.37	84.61 \pm 0.50	84.39 \pm 0.39	96.65 \pm 0.09 \dagger	97.86\pm0.23	\uparrow 1.21
		0.2	75.27 \pm 0.83	74.91 \pm 0.30	76.86 \pm 0.52	77.64 \pm 2.51	78.72 \pm 0.34	95.17 \pm 0.34 \dagger	97.34\pm0.22	\uparrow 2.17
		0.3	65.63 \pm 0.58	65.48 \pm 0.42	66.08 \pm 1.00	62.20 \pm 3.01	70.27 \pm 0.40	90.87 \pm 1.75 \dagger	95.84\pm0.34	\uparrow 4.97

label correction to purify noisy samples. With label correction, we can reduce the noise level of the dataset and achieve better transductive performance. These results verify the effectiveness of our method for noisy PLL.

5.3 Noise Robustness

The above inductive and transductive results are based on the best accuracy. Besides the best accuracy, the last accuracy (i.e., the test accuracy of the last epoch) reflects whether the model can prevent fitting noise samples at the end of training. To reveal the noise robustness of our method, we further compare the last accuracy with and without correction (see Table 4). In this section, we treat the system without correction as the comparison system.

- **With correction:** It is our method that integrates ARNet with PiCO for noisy PLL (see Section 4.3).
- **Without correction:** It comes from our method but omits ARNet. Therefore, this model is identical to PiCO and does not exploit label correction.

In Table 4, we present the performance gap between the best accuracy and the last accuracy. It is important to highlight that we can achieve similar best and last performance in the presence of label noise. Taking the results on MNIST as an example, the gap of our method is only 0.10%~0.15%, while the gap of the comparison system is 8.59%~17.29%. These results indicate that our label correction strategy can improve the noise robustness of existing PLL systems.

Meanwhile, we visualize the curves of noise level and test accuracy in Fig. 5. Without correction, the model fits

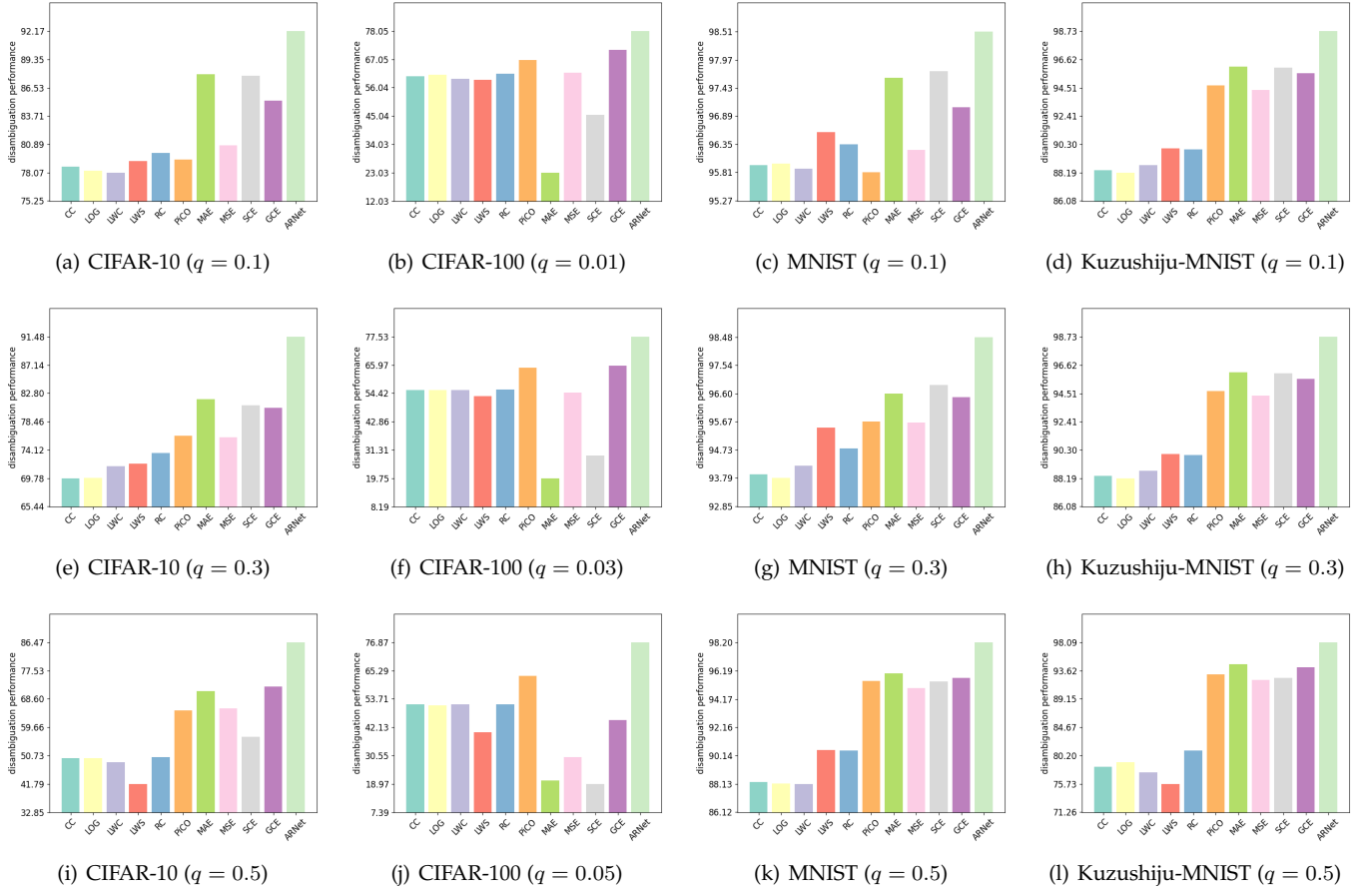


Fig. 4. Transductive performance comparison under different ambiguity levels. The noise level of these datasets is fixed to $\eta = 0.3$.

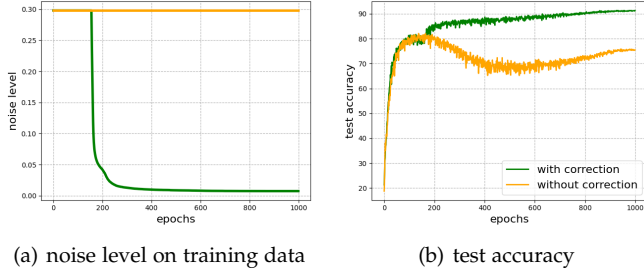


Fig. 5. Performance comparison on CIFAR-10 ($q = 0.3, \eta = 0.3$) with and without correction.

noisy samples during training and causes performance degradation on the test set. Differently, our method can continuously reduce the noise level of the dataset (see Fig. 5(a)), thereby continuously improving the test accuracy under noise conditions (see Fig. 5(b)). These results demonstrate the noise robustness of our proposed method.

5.4 Importance of Augmentation

ARNet uses data augmentation to reduce prediction errors in noisy sample detection and label correction. To reveal the importance of data augmentation, we compare the performance of different combinations of weak (i.e., SimAugment

[50]) and strong (i.e., RandAugment [51]) augmentations. Experimental results are presented in Table 5.

From Table 5, we observe that data augmentation can improve classification performance. Taking the results on CIFAR-10 as an example, the system with data augmentation outperforms the system without data augmentation by 0.50%~2.28%. With the help of data augmentation, we can leverage stricter criteria to select noisy samples, thereby increasing the reliability of predictions. These results demonstrate the importance of data augmentation in noisy PLL.

Meanwhile, we study the impact of different augmentation strategies. From Table 5, we observe that weak augmentation can achieve better performance than strong augmentation. This phenomenon indicates that strong augmentation may not preserve all necessary information for classification. More notably, increasing the number of augmentations does not always result in better performance. More augmentations make the selection of noisy samples more stringent and the prediction results more credible. However, some noise samples may not be corrected due to these strict rules. Therefore, there is a trade-off between them. Strict rules lead to some noisy samples not being corrected, while loose rules lead to some clean samples being wrongly corrected. We need to find an appropriate augmentation strategy.

In Table 6, we further compare the complexity of different strategies. Data augmentation requires additional feed-forward on augmented samples, resulting in more compu-

TABLE 3

Inductive performance comparison with various noisy PLL methods under varying ambiguity levels. The noise level of these datasets is fixed to $\eta = 0.3$. The best performance is highlighted in bold, and the second-highest result is labeled by \dagger .

Dataset	Method	$q = 0.1$	$q = 0.3$	$q = 0.5$
CIFAR-10	MAE	89.82 \dagger	86.71 \dagger	76.42
	MSE	86.16	82.44	71.25
	SCE	89.04	84.42	59.45
	GCE	88.77	85.98	77.95 \dagger
	ARNet	92.04	91.35	86.19
MNIST	MAE	99.20 \dagger	99.10 \dagger	98.83 \dagger
	MSE	99.09	98.94	98.66
	SCE	99.14	99.01	98.60
	GCE	99.18	99.03	98.74
	ARNet	99.23	99.23	99.12
Kuzushiji-MNIST	MAE	97.38	96.52 \dagger	93.20 \dagger
	MSE	96.59	95.03	86.87
	SCE	97.30	96.09	89.30
	GCE	97.51 \dagger	96.16	92.55
	ARNet	97.95	97.87	95.84
Dataset	Method	$q = 0.01$	$q = 0.03$	$q = 0.05$
CIFAR-100	MAE	21.97	18.27	19.26
	MSE	57.09	51.47	29.26
	SCE	40.47	27.00	18.63
	GCE	62.13 \dagger	57.95 \dagger	41.23 \dagger
	ARNet	68.77	68.18	68.09

TABLE 4

Test accuracy with and without correction under different ambiguity levels. The noise level of these datasets is fixed to $\eta = 0.3$. Besides the best accuracy, we also show the test accuracy of the last epoch. The column with Δ shows the gap between the best and last results.

Dataset	q	with correction			without correction		
		Best	Last	Δ	Best	Last	Δ
CIFAR-10	0.1	92.04	91.95	0.09	84.96	77.94	7.02
	0.3	91.35	91.14	0.21	82.25	74.76	7.49
	0.5	86.19	85.89	0.30	68.75	66.64	2.11
CIFAR-100	0.01	68.77	68.49	0.28	58.97	54.55	4.42
	0.03	68.18	67.81	0.37	58.64	53.22	5.42
	0.05	68.09	67.75	0.34	58.18	52.81	5.37
MNIST	0.1	99.23	99.13	0.10	99.00	90.41	8.59
	0.3	99.23	99.12	0.11	98.92	88.32	10.60
	0.5	99.12	98.97	0.15	98.70	81.41	17.29
Kuzushiji-MNIST	0.1	97.95	97.81	0.14	96.53	87.11	9.42
	0.3	97.87	97.75	0.12	95.34	85.06	10.28
	0.5	95.84	95.71	0.13	90.87	78.41	12.46

tational cost and training time. Since feedforward does not change the model architecture, the number of parameters remains the same. Considering the fact that increasing the number of augmentations does not always lead to better performance, we use one weak augmentation to speed up training and improve performance under noisy conditions.

5.5 Parameter Sensitivity

ARNet mainly contains two hyper-parameters: the correction epoch e_0 and the margin τ_e . We automatically determine e_0 and manually select τ_e . In this section, we conduct parameter sensitivity analysis to reveal the impact of these hyper-parameters. Experimental results are shown in Fig. 6.

TABLE 5

Test accuracy of different augmentation strategies under varying ambiguity levels. The noise level of these datasets is fixed to $\eta = 0.3$. In this table, #W denotes the number of weak augmentations and #S denotes the number of strong augmentations.

Dataset	#W	#S	$q = 0.1$	$q = 0.3$	$q = 0.5$
CIFAR-10	0	0	90.37	89.87	86.51
	0	1	90.73	90.30	85.44
	1	0	92.04	91.35	86.19
	0	2	91.40	89.32	84.93
	1	1	92.16	91.32	85.94
	2	0	92.65	91.49	87.01
Dataset	#W	#S	$q = 0.01$	$q = 0.03$	$q = 0.05$
CIFAR-100	0	0	65.40	63.93	62.88
	0	1	67.03	65.63	65.70
	1	0	68.77	68.18	68.09
	0	2	61.70	59.58	58.94
	1	1	66.32	65.13	63.46
	2	0	69.44	68.03	66.90

TABLE 6

Complexity comparison of different augmentation strategies on CIFAR-10. In this table, we compare them in terms of MACs, number of parameters, training time per sample and GPU memory usage.

#W+#S	MACs (G)	Parameters (M)	Training Time (ms)	GPU Memory (GB)
0	1.11	23.01	1.08	3.39
1	1.67	23.01	1.18	4.05
2	2.23	23.01	1.25	4.85

From Fig. 6, we observe that ARNet performs poorly when τ_e is too large or too small. A large τ_e makes the selection of noisy samples strict, causing some noisy samples to be uncorrected. A small τ_e makes the selection of noisy samples easy, causing some clean samples to be wrongly corrected. Therefore, a good choice of τ_e can improve the classification performance under noisy conditions.

Meanwhile, we analyze the influence of e_0 under the optimal τ_e . In Fig. 6(b) and Fig. 6(d), the automatically determined e_0 is 164 and 140, respectively. We also compare with e_0 in $\{1, 100, 200, 300, 400, 500\}$. The performance of ARNet depends on two key modules: noisy sample detection and label correction. Since these modules perform poorly at the early or late epochs (see Fig. 2(a)~2(b)), the classification performance first increases and then decreases with increasing e_0 . More notably, our automatic selection strategy can achieve competitive performance with less manual effort. These results demonstrate the effectiveness of our method.

5.6 Role of Swapping

ARNet corrects the noisy sample by moving its ground-truth label from the non-candidate set to the candidate set. It leads to an increase in the number of candidate labels $|S(x)|$ and the ambiguity level q . Previous works have demonstrated that a large q may increase the difficulty of model optimization, resulting in a decrease in classification performance [27]. To keep $|S(x)|$ consistent, a heuristic solution is to further move out the candidate label with the lowest confidence (i.e., $\bar{y} = \arg \min_{j \in S(x)} f_j(x)$). To sum up,

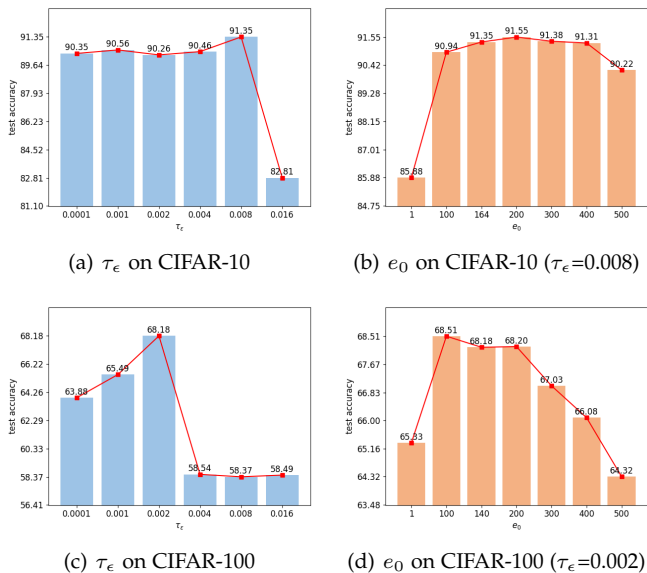


Fig. 6. Parameter sensitivity analysis on CIFAR-10 ($q = 0.3$) and CIFAR-100 ($q = 0.03$). The noise level of these datasets is fixed to $\eta = 0.3$.

TABLE 7

Test accuracy with and without swapping under varying ambiguity levels. The noise level of these datasets is fixed to $\eta = 0.3$.

Dataset	q	with swapping	without swapping
CIFAR-10	0.1	91.18	92.04
	0.3	90.65	91.35
	0.5	84.15	86.19
CIFAR-100	0.01	67.62	68.77
	0.03	67.57	68.18
	0.05	67.19	68.09

we move the ground-truth label into $S(x)$ and move \bar{y} out of $S(x)$ for each noisy sample. We call this strategy *swapping*. To study the role of swapping, we conduct additional experiments in Table 7. The system without swapping is identical to ARNet.

Experimental results in Table 7 demonstrate that swapping does not improve classification performance. Taking the results on CIFAR-10 as an example, the system with swapping performs slightly worse than the system without swapping by 0.70%~2.04%. For noisy samples, swapping can keep the number of candidate labels consistent by moving \bar{y} out of $S(x)$. However, the predictions of ARNet are not completely correct. It may move the ground-truth label out of $S(x)$ due to wrong predictions. Therefore, we do not utilize swapping in this paper.

5.7 Visualization of Embedding Space

In addition to quantitative results, we also conduct qualitative analysis to reveal the strengths of our method. In Figure 7, we visualize the latent representation of different approaches. We exploit t-distributed stochastic neighbor embedding (t-SNE) [52], a technique widely used for high-dimensional data visualization. Experimental results show that our ARNet can effectively disentangle the latent representation and reveal the underlying class distribution. In

Figure 8, we further visualize the latent representation of ARNet with increasing training epochs. From this figure, we observe that the separation among classes becomes clear as the training epoch increases. These qualitative results also verify the effectiveness of our method in noisy PLL.

6 CONCLUSIONS

In this paper, we study the problem of noisy PLL and propose a novel framework ARNet. Unlike existing works that assume the ground-truth label of each sample must reside in the candidate set, we relax this assumption and focus on a more general problem, noisy PLL. To address this problem, we propose ARNet to purify noisy samples and reduce the noise level of the dataset. Through quantitative and qualitative analysis, we verify that ARNet outperforms currently advanced approaches in both inductive and transductive performance. Meanwhile, we demonstrate the noise robustness of our method and reveal the importance of data augmentation. Through parameter sensitivity analysis, we further show the impact of different hyper-parameters and prove the effectiveness of our epoch selection strategy.

This paper focuses on the scenario where both clean and noisy samples have their ground-truth labels in a predefined label space. In the future, we will explore some challenging scenarios. For example, there are out-of-distribution samples in the dataset and the ground-truth labels of these samples are outside the label space.

ACKNOWLEDGEMENTS

This work is funded by the National Key Research and Development Plan of China under Grant 2017YFC0820602 and the National Natural Science Foundation of China (NSFC) under Grants 61771472, 61773379, 61831022 and 62201572.

REFERENCES

- [1] Y. Yan and Y. Guo, "Partial label learning with batch label correction," in *Proceedings of the AAAI Conference on Artificial Intelligence*, 2020, pp. 6575–6582.
- [2] F. Zhang, L. Feng, B. Han, T. Liu, G. Niu, T. Qin, and M. Sugiyama, "Exploiting class activation value for partial-label learning," in *International Conference on Learning Representations*, 2021, pp. 1–17.
- [3] Y.-C. Chen, V. M. Patel, R. Chellappa, and P. J. Phillips, "Ambiguously labeled learning using dictionaries," *IEEE Transactions on Information Forensics and Security*, vol. 9, no. 12, pp. 2076–2088, 2014.
- [4] Y. Yao, J. Deng, X. Chen, C. Gong, J. Wu, and J. Yang, "Deep discriminative cnn with temporal ensembling for ambiguously-labeled image classification," in *Proceedings of the AAAI Conference on Artificial Intelligence*, 2020, pp. 12 669–12 676.
- [5] L. Liu and T. Dietterich, "Learnability of the superset label learning problem," in *International Conference on Machine Learning*, 2014, pp. 1629–1637.
- [6] E. Hüllermeier and W. Cheng, "Superset learning based on generalized loss minimization," in *Joint European Conference on Machine Learning and Knowledge Discovery in Databases*, 2015, pp. 260–275.
- [7] M. J. Huiskes and M. S. Lew, "The mir flickr retrieval evaluation," in *Proceedings of the 1st ACM International Conference on Multimedia Information Retrieval*, 2008, pp. 39–43.
- [8] L. Liu and T. Dietterich, "A conditional multinomial mixture model for superset label learning," *Advances in neural information processing systems*, vol. 25, 2012.
- [9] F. Briggs, X. Z. Fern, and R. Raich, "Rank-loss support instance machines for miml instance annotation," in *Proceedings of the 18th ACM SIGKDD international conference on Knowledge discovery and data mining*, 2012, pp. 534–542.



Fig. 7. T-SNE visualization results of different methods on the CIFAR-10 test set ($q = 0.3, \eta = 0.3$).

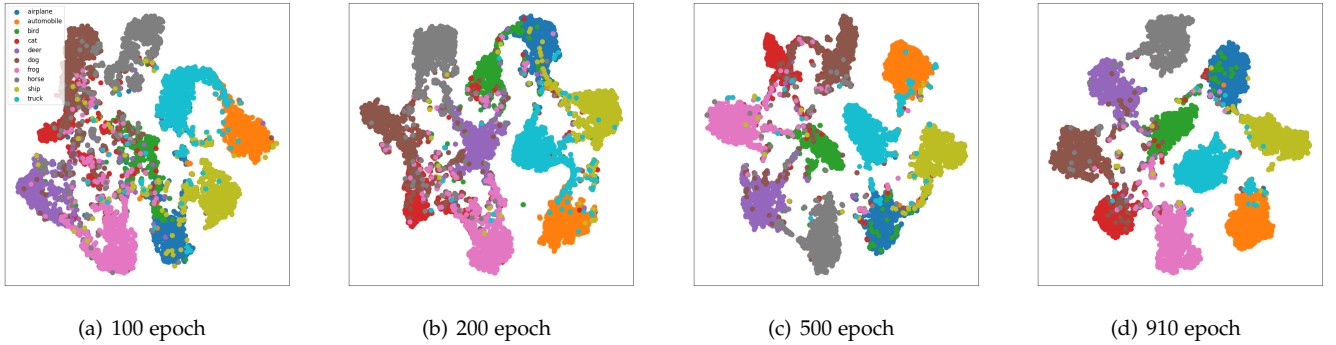


Fig. 8. T-SNE visualization results of ARNet on the CIFAR-10 test set ($q = 0.3, \eta = 0.3$) with increasing training epochs.

- [10] L. Feng and B. An, "Leveraging latent label distributions for partial label learning," in *IJCAI*, 2018, pp. 2107–2113.
- [11] N. Xu, C. Qiao, X. Geng, and M.-L. Zhang, "Instance-dependent partial label learning," *Advances in Neural Information Processing Systems*, pp. 27 119–27 130, 2021.
- [12] T. Cour, B. Sapp, C. Jordan, and B. Taskar, "Learning from ambiguously labeled images," in *IEEE Conference on Computer Vision and Pattern Recognition*, 2009, pp. 919–926.
- [13] E. Hüllermeier and J. Beringer, "Learning from ambiguously labeled examples," *Intelligent Data Analysis*, vol. 10, no. 5, pp. 419–439, 2006.
- [14] D.-D. Wu, D.-B. Wang, and M.-L. Zhang, "Revisiting consistency regularization for deep partial label learning," in *International Conference on Machine Learning*, 2022, pp. 24 212–24 225.
- [15] S.-Y. Xia, J. Lv, N. Xu, and X. Geng, "Ambiguity-induced contrastive learning for instance-dependent partial label learning," in *Proceedings of the Thirty-First International Joint Conference on Artificial Intelligence, IJCAI*, 2022, pp. 3615–3621.
- [16] N. Nguyen and R. Caruana, "Classification with partial labels," in *Proceedings of the 14th ACM SIGKDD international conference on Knowledge discovery and data mining*, 2008, pp. 551–559.
- [17] F. Yu and M.-L. Zhang, "Maximum margin partial label learning," in *Asian conference on machine learning*, 2016, pp. 96–111.
- [18] R. Jin and Z. Ghahramani, "Learning with multiple labels," in *Proceedings of the 15th International Conference on Neural Information Processing Systems*, 2002, pp. 921–928.
- [19] J. Cid-Sueiro, "Proper losses for learning from partial labels," in *Proceedings of the 25th International Conference on Neural Information Processing Systems-Volume 1*, 2012, pp. 1565–1573.
- [20] J. Lv, L. Feng, M. Xu, B. An, G. Niu, X. Geng, and M. Sugiyama, "On the robustness of average losses for partial-label learning," *arXiv preprint arXiv:2106.06152*, 2021.
- [21] T. Cour, B. Sapp, and B. Taskar, "Learning from partial labels," *The Journal of Machine Learning Research*, vol. 12, pp. 1501–1536, 2011.
- [22] C.-Z. Tang and M.-L. Zhang, "Confidence-rated discriminative partial label learning," in *Proceedings of the Thirty-First AAAI Conference on Artificial Intelligence*, 2017, pp. 2611–2617.
- [23] M.-L. Zhang and F. Yu, "Solving the partial label learning problem: An instance-based approach," in *Twenty-fourth international joint conference on artificial intelligence*, 2015.

- [24] M.-L. Zhang, B.-B. Zhou, and X.-Y. Liu, "Partial label learning via feature-aware disambiguation," in *Proceedings of the 22nd ACM SIGKDD international conference on knowledge discovery and data mining*, 2016, pp. 1335–1344.
- [25] C. Gong, T. Liu, Y. Tang, J. Yang, J. Yang, and D. Tao, "A regularization approach for instance-based superset label learning," *IEEE Transactions on Cybernetics*, vol. 48, no. 3, pp. 967–978, 2017.
- [26] J. Lv, M. Xu, L. Feng, G. Niu, X. Geng, and M. Sugiyama, "Progressive identification of true labels for partial-label learning," in *International Conference on Machine Learning*. PMLR, 2020, pp. 6500–6510.
- [27] L. Feng, J. Lv, B. Han, M. Xu, G. Niu, X. Geng, B. An, and M. Sugiyama, "Provably consistent partial-label learning," *Advances in Neural Information Processing Systems*, vol. 33, pp. 10948–10960, 2020.
- [28] H. Wen, J. Cui, H. Hang, J. Liu, Y. Wang, and Z. Lin, "Leveraged weighted loss for partial label learning," in *International Conference on Machine Learning*. PMLR, 2021, pp. 11 091–11 100.
- [29] H. Wang, R. Xiao, Y. Li, L. Feng, G. Niu, G. Chen, and J. Zhao, "Pico: Contrastive label disambiguation for partial label learning," in *International Conference on Learning Representations*, 2022, pp. 1–18.
- [30] D. Hendrycks and K. Gimpel, "A baseline for detecting misclassified and out-of-distribution examples in neural networks," in *International Conference on Learning Representations*, 2017, pp. 1–12.
- [31] S. Liang, Y. Li, and R. Srikant, "Enhancing the reliability of out-of-distribution image detection in neural networks," in *International Conference on Learning Representations*, 2018, pp. 1–27.
- [32] A. Krizhevsky, "Learning multiple layers of features from tiny images," University of Toronto, Tech. Rep., 2009.
- [33] P. E. Hart, D. G. Stork, and R. O. Duda, *Pattern classification*. Wiley Hoboken, 2000.
- [34] N. Xu, J. Lv, and X. Geng, "Partial label learning via label enhancement," in *Proceedings of the AAAI Conference on Artificial Intelligence*, 2019, pp. 5557–5564.
- [35] L. Jiang, Z. Zhou, T. Leung, L.-J. Li, and L. Fei-Fei, "Mentornet: Learning data-driven curriculum for very deep neural networks on corrupted labels," in *International conference on machine learning*, 2018, pp. 2304–2313.
- [36] E. Arazo, D. Ortego, P. Albert, N. O'Connor, and K. McGuinness, "Unsupervised label noise modeling and loss correction," in *International conference on machine learning*, 2019, pp. 312–321.
- [37] J. Li, R. Socher, and S. C. Hoi, "Dividemix: Learning with noisy labels as semi-supervised learning," in *International Conference on Learning Representations*, 2019, pp. 1–14.
- [38] H. Permuter, J. Francos, and I. Jermyn, "A study of gaussian mixture models of color and texture features for image classification and segmentation," *Pattern recognition*, vol. 39, no. 4, pp. 695–706, 2006.
- [39] Y. Zhang, S. Zheng, P. Wu, M. Goswami, and C. Chen, "Learning with feature-dependent label noise: A progressive approach," in *International Conference on Learning Representations*, 2021, pp. 1–13.
- [40] N. Xu, J. Lv, B. Liu, C. Qiao, and X. Geng, "Progressive purification for instance-dependent partial label learning," *arXiv preprint arXiv:2206.00830*, 2022.
- [41] Y. LeCun, L. Bottou, Y. Bengio, and P. Haffner, "Gradient-based learning applied to document recognition," *Proceedings of the IEEE*, vol. 86, no. 11, pp. 2278–2324, 1998.
- [42] T. Clanuwat, M. Bober-Irizar, A. Kitamoto, A. Lamb, K. Yamamoto, and D. Ha, "Deep learning for classical japanese literature," *arXiv preprint arXiv:1812.01718*, 2018.
- [43] L. Feng, T. Kaneko, B. Han, G. Niu, B. An, and M. Sugiyama, "Learning with multiple complementary labels," in *International Conference on Machine Learning*. PMLR, 2020, pp. 3072–3081.
- [44] A. Ghosh, H. Kumar, and P. S. Sastry, "Robust loss functions under label noise for deep neural networks," in *Proceedings of the AAAI conference on artificial intelligence*, vol. 31, no. 1, 2017.
- [45] Y. Wang, X. Ma, Z. Chen, Y. Luo, J. Yi, and J. Bailey, "Symmetric cross entropy for robust learning with noisy labels," in *Proceedings of the IEEE/CVF International Conference on Computer Vision*, 2019, pp. 322–330.
- [46] Z. Zhang and M. R. Sabuncu, "Generalized cross entropy loss for training deep neural networks with noisy labels," in *Proceedings of the 32nd International Conference on Neural Information Processing Systems*, 2018, pp. 8792–8802.
- [47] A. Paszke, S. Gross, F. Massa, A. Lerer, J. Bradbury, G. Chanan, T. Killeen, Z. Lin, N. Gimelshein, L. Antiga *et al.*, "Pytorch: an imperative style, high-performance deep learning library," in *Proceedings of the 33rd International Conference on Neural Information Processing Systems*, 2019, pp. 8026–8037.

- [48] G. Lyu, S. Feng, T. Wang, C. Lang, and Y. Li, "Gm-pll: graph matching based partial label learning," *IEEE Transactions on Knowledge and Data Engineering*, vol. 33, no. 2, pp. 521–535, 2019.
- [49] D.-B. Wang, M.-L. Zhang, and L. Li, "Adaptive graph guided disambiguation for partial label learning," *IEEE Transactions on Pattern Analysis and Machine Intelligence*, 2021.
- [50] P. Khosla, P. Teterwak, C. Wang, A. Sarna, Y. Tian, P. Isola, A. Maschinot, C. Liu, and D. Krishnan, "Supervised contrastive learning," *Advances in Neural Information Processing Systems*, vol. 33, pp. 18661–18 673, 2020.
- [51] E. D. Cubuk, B. Zoph, J. Shlens, and Q. V. Le, "RandAugment: Practical data augmentation with no separate search," *arXiv preprint arXiv:1909.13719*, vol. 2, no. 4, p. 7, 2019.
- [52] L. Van der Maaten and G. Hinton, "Visualizing data using t-sne," *Journal of machine learning research*, vol. 9, pp. 2579–2605, 2008.



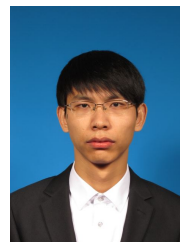
Zheng Lian received the B.S. degree from the Beijing University of Posts and Telecommunications, Beijing, China, in 2016. And he received the Ph.D degree from the Institute of Automation, Chinese Academy of Sciences, Beijing, China, in 2021. He is currently an Assistant Professor at National Laboratory of Pattern Recognition, Institute of Automation, Chinese Academy of Sciences, Beijing, China. His current research interests include affective computing, noisy-label learning and partial label learning.



Mingyu Xu received the B.S. degree from Peking University, Beijing, China, in 2021. He is currently working toward the M.S. degree with the Institute of Automation, Chinese Academy of Sciences, Beijing, China. His current research interests include affective computing, uncertainty learning and deep learning.



Lan Chen received the B.S. degree from the China University of Petroleum, Beijing, China, in 2016. And she received the Ph.D degree from the Institute of Automation, Chinese Academy of Sciences, Beijing, China, in 2022. Her current research interests include computer graphics and image processing.



Licai Sun received the B.S. degree from Beijing Forestry University, Beijing, China, in 2016, and the M.S. degree from University of Chinese Academy of Sciences, Beijing, China, in 2019. He is currently working toward the Ph.D degree with the School of Artificial Intelligence, University of Chinese Academy of Sciences, Beijing, China. His current research interests include affective computing, deep learning and multimodal representation learning.



Bin Liu received his the B.S. degree and the M.S. degree from Beijing institute of technology, Beijing, China, in 2007 and 2009 respectively. He received Ph.D. degree from the National Laboratory of Pattern Recognition, Institute of Automation, Chinese Academy of Sciences, Beijing, China, in 2015. He is currently an Associate Professor in the National Laboratory of Pattern Recognition, Institute of Automation, Chinese Academy of Sciences, Beijing, China. His current research interests include affective computing and audio signal processing.



Jianhua Tao received the Ph.D. degree from Tsinghua University, Beijing, China, in 2001, and the M.S. degree from Nanjing University, Nanjing, China, in 1996. He is currently a Professor with National Laboratory of Pattern Recognition, Institute of Automation, Chinese Academy of Sciences, Beijing, China. He has authored or coauthored more than eighty papers on major journals and proceedings. His current research interests include speech recognition, speech synthesis and coding methods,

human-computer interaction, multimedia information processing, and pattern recognition. He is the Chair or Program Committee Member for several major conferences, including ICPR, ACII, ICMI, ISCSLP, etc. He is also the Steering Committee Member for the IEEE Transactions on Affective Computing, an Associate Editor for Journal on Multimodal User Interface and International Journal on Synthetic Emotions, and the Deputy Editor-in-Chief for Chinese Journal of Phonetics.